162. Conversion of Light into Electricity with Trinuclear Ruthenium Complexes Adsorbed on Textured TiO_2 Films

by **Mohammad K. Nazeeruddin, Paul Liska, Jacques Moser, Nick Vlachopoulos,** and **Michael Grätzel***

Institut de Chimie Physique, Ecole Polytechnique Fédérale, CH-1015 Lausanne

(11.IV.90)

A series of CN-bridged trinuclear Ru complexes of the general structure $[RuL_2(\mu\text{-}(CN)Ru(CN)L'_2)_2]$ where L is 2,2′-bipyridine-4,4′-dicarboxylic acid and L′ is 2,2′-bipyridine (**1**) 2,2′-bipyridine-4,4′-dicarboxylic acid (**2**), 4,4′-dimethyl-2,2′-bipyridine (**3**), 4,4′-diphenyl-2,2′-bipyridine (**4**), 1,10-phenanthroline (**5**), and bathophenanthrolinedisulfonic acid (**6**) have been synthesized, and their spectral and electrochemical properties investigated. The two carboxylic functions on the 2,2′-bipyridine ligand L serve as interlocking groups through which the dye is attached at the surface of TiO_2 films having a specific surface texture. The role of these interlocking groups is to provide strong electronic coupling between the π^* orbital of the 2,2′-bipyridine and the 3d-wave-function manifold of the conduction band of the TiO_2, allowing the charge injection to proceed at quantum yields close to 100%. The charge injection and recombination dynamics have been studied with colloidal TiO_2, using laser photolysis technique in conjunction with time-resolved optical spectroscopy. Photocurrent action spectra obtained from photo-electrochemical experiments with these trinuclear complexes cover a very broad range in the visible, making them attractive candidates for solar light harvesting. Monochromatic incident photon-to-current conversion efficiencies are strikingly high exceeding 80% in some cases. Performance characteristics of regenerative cells operating with these trinuclear complexes and ethanolic triiodide/iodide redox electrolyte have been investigated. Optimal results were obtained with complex **1** which gave a fill factor of 75% and a power conversion efficiency of 11.3% at 520 nm.

Introduction. – The worldwide quest to develop clean and renewable energy resources has stimulated a major effort in the field of photovoltaic cells. Apart from the conventional dry cells based mostly on silicon technology, electricity can be produced from sunlight also by photo-electrochemical devices [1]. These studies have mainly employed single-crystal semiconductors as light harvesting units whose price is prohibitively high for practical development. One alternative and much cheaper approach is to make use of dye-sensitized, large band-gap semiconductor films to absorb solar light [2]. In such a device, a dye stuff (sensitizer) absorbs visible light and, after excitation, injects electrons in the conduction band of the semiconductor producing an electric current. The difficulties in obtaining reasonable conversion efficiencies with such systems are notorious. Apart from poor injection quantum yields, the light absorption by a monolayer of sensitizer adsorbed on a flat surface is at best a few percent. Multilayer deposition has proved to be an unsuccessful approach to solve this dilemma due to the lack of photoactivity and the filtering effect of the dye molecules which are not in direct contact with the semiconductor.

A recent unexpected breakthrough in this field is the discovery [3–8] that TiO_2 films with a specific fractal-type surface texture [9] can be sensitized with strikingly high yields. Incident photon-to-current conversion efficiencies exceeding 70% have been obtained in several cases. The clue to obtain such high efficiencies is to endow the sensitizer with suitable interlocking groups which serve as electronic bridging function between its chromophoric moiety and the conduction band of the TiO_2 [7] [8].

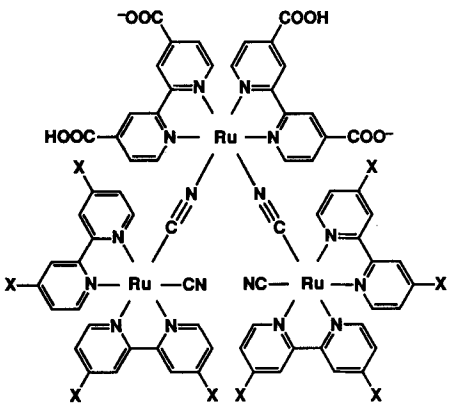

1 X = H
2 X = COOH
3 X = Me
4 X = Ph

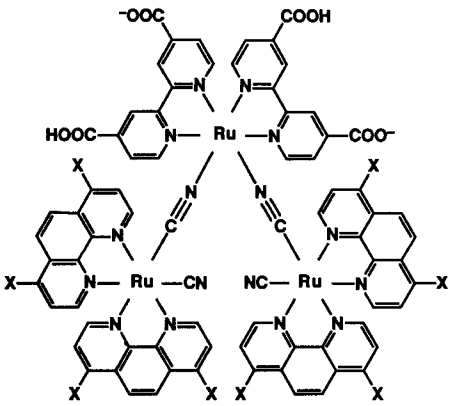

5 X = H
6 X = $C_6H_4SO_3^-$

Here, we report investigations on the performance of CN-bridged trinuclear Ru complexes **1**–**6** as sensitizers for these newly developed TiO_2 films. This class of compounds is novel, and only a few reports concerning the photophysical and redox properties of such polynuclear complexes have appeared so far [10]. *Scandola* has conceived a possible antenna effect in the light-harvesting process by such sensitizers which should render them effective even on relatively smooth surfaces [11]. The present results show that trinuclear Ru complexes show promising features when adsorbed onto rough TiO_2 films, both with respect to efficiency of light-energy conversion as well as from their stability under long-term illumination.

Experimental. – **Materials.** – The ligands 2,2′-bipyridine (*Fluka*), 2,2′-bipyridine-4,4′-dicarboxylic acid (*Alfa*), 4,4′-dimethyl-2,2′-bipyridine (*Fluka*), 4,4′-diphenyl-2,2′-bipyridine (*Aldrich*), 1,10-phenanthroline, and bathophenanthrolinedisulfonic acid, and $RuCl_3 \cdot 3H_2O$ from *Fluka* were commercial samples and were used without further purification. All other materials were of reagent grade and were used as received. *cis*-Dichlorobis(2,2′-bipyridine-4,4′-dicarboxylic acid) Ru(II) was synthesized as described in [8].

1. *Synthesis of* cis-*[Ru(II)(CN)$_2$L′$_2$]* (L′ = 2,2′-bipyridine, 2,2′-bipyridine-4,4′-dicarboxylic acid, 4,4′-dimethyl-2,2′-bipyridine, 4,4′-diphenyl-2,2′-bipyridine, 1,10-phenanthroline, and bathophenanthrolinedisulfonic acid).

In a typical synthesis, where L′ is 2,2′-bipyridine, the previously reported preparation of this complex [10b] was modified as follows: 800 mg (1.45 mmol) of *cis*-dichlorobis(2,2′-bipyridine) was dissolved in 80 ml of DMF, under N_2, in the dark in order to avoid photo-induced *cis*/*trans* isomerization. To this soln., 190 mg (2.91 mmol) of KCN, which was separately dissolved in H_2O, was added. The soln. was heated at reflux for 3 h. During the course of reaction, the dark-purple color changed to an orange-red. The progress of this reaction was monitored with the help of UV/VIS spectrophotometer. The soln. was filtered through a fine glass frit, and the filtrate was evaporated to dryness under reduced pressure. The residue was dissolved in 20 ml of H_2O and filtered in order to remove any unreacted starting complex. Again, the filtrate was evaporated to dryness. The resulting residue was dissolved in 15 ml of EtOH and filtered through a fine glass frit which removed quantitatively the KCl produced. To the filtrate, 150 ml of Et_2O was added. The turbid soln. was placed in a refrigerator for 2 h, after which time the precipitate was collected by filtration onto a glass frit. The precipitate was washed with 3 × 5 ml portions of EtOH/Et_2O 2:10, followed by anh. Et_2O and dried *in vacuo*: yield 0.62 g (90%). The purity of this complex was checked by elemental analysis and luminescence behavior. Other complexes with L′ = 2,2′-bipyridine-4,4′-dicarboxylic acid, 4,4′-dimethyl-2,2′-bipyridine, 4,4′-diphenyl-2,2′-bipyridine, 1,10-phenanthroline, and bathophenanthrolinedisulfonic acid have been synthesized in an analogous way.

2. *Synthesis of* cis-*Dicyanobis(2,2′-bipyridine-4,4′-dicarboxylic acid)Ruthenium(II).* This complex was prepared as the previous one except for the isolation and purification. After refluxing the reactants *cis*-[Ru(4,4′-COOH-2,2′-bpy)$_2$Cl$_2$] and KCN in 1:2 ratio for 4 h, the soln. was allowed to cool and filtered through a fine glass frit. The filtrate was evaporated to dryness under reduced pressure. The resulting residue was dissolved in H_2O at pH 6–7, and the required complex was isolated as a neutral salt at its isoelectric point, pH 2.6.

3. *Synthesis of CN-Bridged Trinuclear Complexes of Ru(II): [RuL$_2$(μ-(CN)Ru(CN)L′$_2$)$_2$]* (L = 2,2′-bipyridine-4,4′-dicarboxylic acid; L′ = 2,2′-bipyridine, *or* 2,2′-bipyridine-4,4′-dicarboxylic acid, *or* 4,4′-dimethyl-2,2′-bipyridine, *or* 4,4′-diphenyl-2,2′-bipyridine, *or* 1,10-phenanthroline, *or* bathophenanthrolinedisulfonic acid). In a typical synthesis where L = 4,4′-(COOH)$_2$-2,2′-bpy and L′ = 2,2′-bpy, 307 mg (0.43 mmol) of RuL_2Cl_2 was dissolved in 3 ml of aq 1M NaOH, under N_2, in the dark. The soln. was subsequently diluted by adding 30 ml of DMF. To this soln. 400 mg (0.86 mmol) of $RuL_2(CN)_2$ were added. The soln. was heated at reflux for 6 h and allowed to cool to r.t. The soln. was filtered through a fine glass frit, and the filtrate was evaporated to dryness. The resulting residue was dissolved in H_2O at pH 6–7. The pH of this soln. was lowered to 3.2 which produced a dense precipitate. The soln. was placed in a refrigerator for 10 h, after which time the precipitate was collected by filtration onto a glass frit. The precipitate was washed with acetone/Et_2O 2:5 followed by anh. Et_2O and dried *in vacuo:* yield 450 mg (69%). In air, this compound adds 10 lattice H_2O molecules as shown by elemental analysis (calc. values are in parenthesis): C 47.75 (48.00); H 3.89 (4.03); N 12.99 (13.17); H_2O 10.48. The C/N ratio of 4.25 (calc. value 4.25) indicates that no decarboxylation took place during the preparation of the trimer.

Trinuclear complexes with L′ = 2,2′-bipyridine-4,4′-dicarboxylic acid, *or* 4,4′-dimethyl-2,2′-bipyridine, *or* 4,4′-diphenyl-2,2′-bipyridine, *or* 1,10-phenanthroline, *or* bathophenanthrolinedisulfonic acid have been synthesized in a similar way.

4. *Preparation of the TiO_2 Films.* The sol-gel method used to prepare the textured TiO_2 films was similar to the procedure described in [7], except that the alcoholic precursor soln. was deposited onto a 2 × 10-cm-sized sheet of conducting glass (*Asahi,* Tokyo, Japan; fluorine-doped SnO_2 deposited on soda lime float glass, thickness 1.1 mm, area resistance *ca.* 10 Ω/square, optical transmission in the VIS *ca.* 80%). In some cases, a dopant (2.5% of magnesium or aluminium oxide) was incorporated in the last layer. After the completion of the TiO_2 deposition, the glass was cut into pieces of 0.8-cm width and 2-cm length. Of the 2 cm, only *ca.* 1.5 were covered with the TiO_2. The remaining area was protected during film deposition to leave bare conducting glass surface exposed for electric contacting. In this fashion, 12 *ca.* 1.2-cm^2-sized TiO_2 electrodes were obtained originating from the same film preparation. These TiO_2 electrodes are expected to have similar surface morphology and composition facilitating the comparison of the performance characteristics of the different trinuclear complexes.

After finishing the deposition of the TiO_2 layers and annealing them at 550°, they were immediately coated with the trinuclear Ru complexes **1**–**6**. Monomolecular coatings were formed by dipping the electrode in an alcoholic or aq. soln. of the sensitizer. This procedure was investigated in detail for **1** and **2** for which immersion of the TiO_2 electrodes during 1 h in a 10^{-4}M soln. of the complex in EtOH gave satisfactory results with good reproducibility. Longer exposure of the films to the soln. or higher dye concentrations resulted in the deposition of multilayers decreasing the charge-injection yields. The formation of such multilayers was examinated by luminescence analysis of dry TiO_2 films after dye adsorption. (In the presence of multilayers, the red emission of the trimer is strongly enhanced, since the first monolayer of trimer exhibits practically no luminescence due to very efficient electron-transfer quenching by the TiO_2 substrate.) Similarly, the complexes **3**–**6** were deposited from 5×10^{-4}M aq. solns. of pH 3.5–4.

5. *Preparation of TiO_2 Sols in EtOH.* Ti(IV)$(EtO)_4$ (10 ml, *Alfa*) was added dropwise to 150 ml of abs. EtOH acidified by 0.5 ml of conc. HCl and cooled to ~ 0°. The opaque suspension was stirred for *ca.* 1 h up to the total dissolution of the polymeric chains. The clear soln. was again cooled to 0°, and 3 ml of H_2O were added. After 2–3 h of stirring at r.t., the light yellow color disappeared completely. The colorless colloid, consisting mainly of amorphous TiO_2, was then boiled under reflux for 90 h. The concentration of the oxide was determined gravimetrically to be typically 6 g/l. Application of quasi-elastic light scattering yields for the hydrodynamic radius of the particles values ranging from 5 to 10 nm.

Methods. – The photocurrent potential characteristics were measured using a Xe arc light source and a *Wenkin* potentiostat (*Bank Electronic GmbH,* FRG). The photocurrent action spectrum was obtained with a *Bausch & Lomb* 500-nm blaze high-intensity monochromator. The monochromatic photon flux impinging on the cell was determined by a *YSI Kettering* model *65-A* radiometer. This agreed, within 5%, with the values measured by ferrioxalate actinometry. The electrochemical system employed a single-compartment, three-electrode cell, with a Pt counterelectrode and a suitable aq. reference system, *e.g.* Ag/AgCl, Hg/Hg_2SO_4 or Hg/Hg_2Cl_2 (sat. calomel

electrode, SCE) in addition to the TiO_2 surface under investigation. All potentials are reported *vs.* SCE. The regenerative photoelectrochemical cell consisted of the dye loaded TiO_2 film deposited on the transparent conductive glass support (surface area between 1 and 2 cm^2) and a conductive glass sheet loaded with a thin Pt film serving as the counterelectrode. A thin film of an alcoholic I_2/I^- electrolyte was attracted from a reservoir into the inter-electrode space by capillary forces. Laser photolysis experiments employed a *Q*-switched, frequency-doubled *Nd-YAG* laser having a pulse width of *ca.* 10 ns. The system used for time-resolved kinetic spectroscopy in the 10^{-8} to 10^0 s domain has been described in [12].

Results and Discussion. – *Photocurrent Action Spectra of TiO_2 Films Coated with Trinuclear Ru Complexes.* Photocurrent action spectra obtained with the TiO_2 films coated with the trinuclear Ru complexes **1–6** are shown in *Figs. 1–3*. The incident monochromatic photon-to-current conversion efficiency (IPCE) defined as the number of electrons generated by light in the external circuit divided by the number of incident photons is plotted as a function of the excitation wavelength. This was obtained from the photocurrents by means of the equation:

$$\text{IPCE [\%]} = \frac{[(1.24 \times 10^3) \times \text{photocurrent density [}\mu\text{A/cm}^2\text{]}]}{[\text{wavelength [nm]} \times \text{photon flux [W/m}^2\text{]}]} \quad (1)$$

These experiments were performed with the sandwich-type regenerative cell configuration in the presence of the alcoholic iodine/iodide redox electrolyte. The photocurrents were obtained under short-circuit conditions where the TiO_2 electrode is poised to a potential of 0.1 V measured against an aqueous saturated calomel reference electrode (SCE). The intensity of the incident monochromatic light was typically in the 0.1–0.2 mW/cm^2 range, and the photocurrents obtained were 20 to 80 $\mu A/cm^2$. The TiO_2 films were illuminated from the front side through the conducting glass support. Except for the dashed line in *Fig. 1*, the spectra reported are uncorrected for the absorption of incident light (*ca.* 20%) by the conducting glass. While the bare TiO_2 films due to the 3.2-eV band

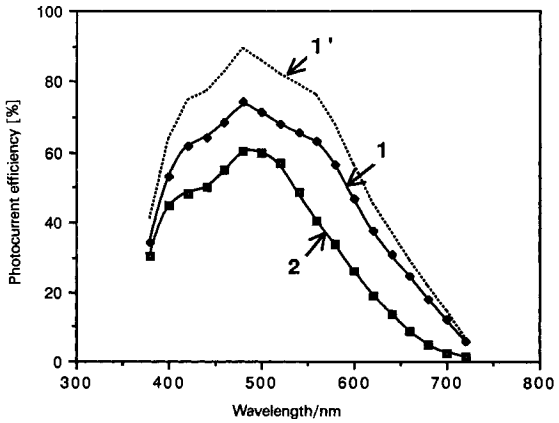

Fig. 1. *Photocurrent action spectra for polycrystalline TiO_2 films coated with the trinuclear Ru complexes* **1** *and* **2**. Spectra were obtained with the thin layer cell containing a solution of 0.1M LiI and 3×10^{-3}M I_2 in EtOH as electrolyte. The dye was excited through the conducting glass sheet serving as support for the TiO_2 film. IPCE is plotted as a function of excitation wavelength. The dashed line *1'* is the photoaction spectrum obtained for **1** corrected for light absorption by the glass support. The size of the working electrode is *ca.* 1.3 cm^2. The counterelectrode was a conducting glass electrode covered with a transparent film of colloidal Pt.

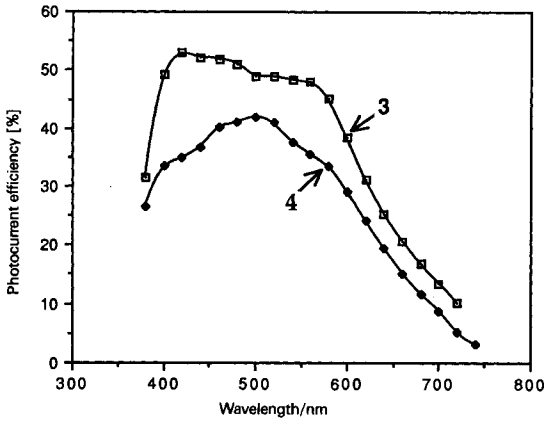

Fig. 2. *Photocurrent action spectra obtained for the trinuclear Ru complexes* **3** *and* **4**. Conditions as in *Fig. 1*.

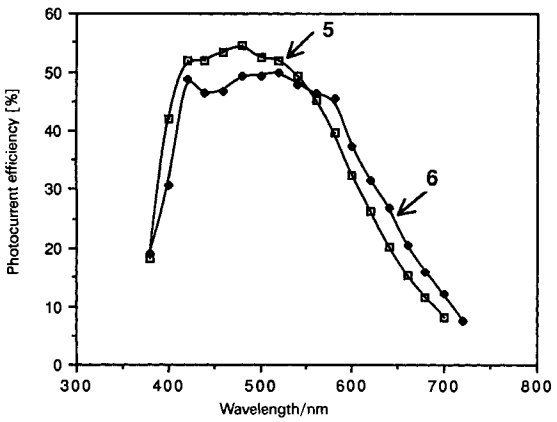

Fig. 3. *Photocurrent action spectra obtained for the trinuclear Ru complexes* **5** *and* **6**. Conditions as in *Fig. 1*.

gap of anatase give practically no photocurrents in the VIS, the response of the electrodes coated with the trinuclear complexes is excellent. Particularly impressive is the IPCE value obtained for sensitizer **1** exceeding 70% around 480 nm. Taking the absorption of light by the conducting glass deposit into account, this corresponds even to 90%. This is the highest incident photon-to-current conversion efficiency observed so far with our textured TiO_2 films. The feature of the action spectrum obtained with **1** is broader than that obtained with **2**. In particular, the former exhibits a shoulder at 550 nm which is absent in the presence of the latter. The tail of the spectrum extends well into the red, the IPCE exceeding still 10% at 700 nm.

The action spectra observed with complexes **3–6** display also a broad feature in the VIS. The photoresponse curve is conspicuously flat for **3** and **6** whose IPCE values remain practically constant at 53% and 50% respectively, in the wavelength domain between 400 and 600 nm before declining towards the red. Such broad features in the action spectrum are unusual for molecular sensitizers resembling more closely the photocurrent response of semiconducting electrodes to band-gap excitation. The current yields observed with complexes **3–6** appear to be somewhat smaller than with **1** and **2**.

Thus, for **3** and **4**, the maximal IPCE values attained in the plateau region are 53% and 42%, while those for **5** and **6** are around 50%. However, the yields obtained in *Figs. 2* and *3* should be considered as lower limits, since the deposition procedure of the sensitizer on the TiO_2 film has not yet been optimized in these cases.

Photophysical and Electrochemical Characterization of Complexes **1** *and* **2** *in Homogeneous Solution.* The promising behavior of the trinuclear Ru complexes as charge-transfer sensitizers at the surface of our textured TiO_2 films warrants more detailed investigations of their photophysical and electrochemical properties. Here, we compare the properties of the complexes **1** and **2**. Results concerning the remaining complexes will be published later.

Fig. 4 presents the absorption and emission spectrum of **1** in EtOH. The absorption maximum in the VIS is located at 478 nm, the decadic extinction coefficient being $1.88 \times 10^4\,M^{-1} \cdot cm^{-1}$. There is also a distinct shoulder appearing at 518 nm. The complex emits in the red with a maximum at 720 nm. The lifetime of the emission is surprisingly long. Time-resolved measurements in deaerated and aerated EtOH yielded $\tau = 360$ ns and 110 ns, respectively.

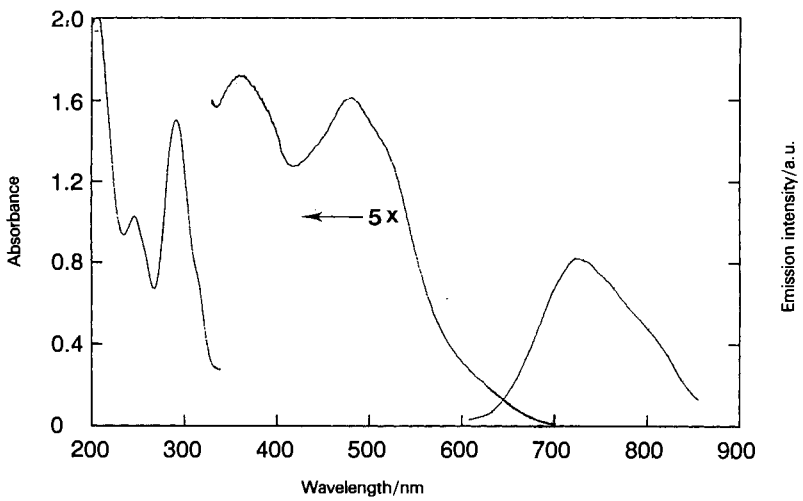

Fig. 4. *Absorption and emission spectrum of a* 2×10^{-5} M *solution of* **1** *in EtOH.* Optical pathlength 1 cm. Excitation wavelength for the emission 532 nm.

The trinuclear complex **2** exhibits absorption and emission features which are different from those displayed by **1**. The absorption maximum in the VIS is located at 480 nm, the extinction coefficient being $2.9 \times 10^4\,M^{-1} \cdot cm^{-1}$. Note also that the shoulder at 518 nm observed for **1** is absent in the case of **2**. The emission spectrum exhibits a broad maximum centered around 700 nm with a luminescence lifetime of 330 ns.

Comparison of *Figs. 1, 4,* and *5* reveals that for both trinuclear complexes the photocurrent action spectrum is shifted towards the red with respect to the absorption spectrum. Note that this displacement is more pronounced for **1** than for **2**. A similar red shift in the photocurrent spectrum has also been observed for a mononuclear carboxylated bipyridine complex of Ru [13], and the effect has been interpreted in terms of an

increase in the delocalization of the π^* orbital of the bipyridine ligand upon adsorption of the complex at the surface of TiO_2. The interaction of the carboxylic group with surface Ti ions is likely to involve formation of C–O–Ti bonds. Thus, the role of the COOH is to serve as an interlocking group coupling electronically the π^* orbitals of the 2,2′-bpy ligand to the Ti(3d)-orbital manifold of the semiconductor. This coupling is rendered efficient by the presence of π electrons in the bridging group and leads to increased delocalization of the π^* level of the 2,2′-bpy ligand. The energy of the π^* level is decreased by this delocalization which explains the observed red shift in the photocurrent action spectrum. Since this shift is more pronounced for **1** as compared to **2**, one concludes that the former exhibits stronger interaction with the TiO_2 surface than the latter.

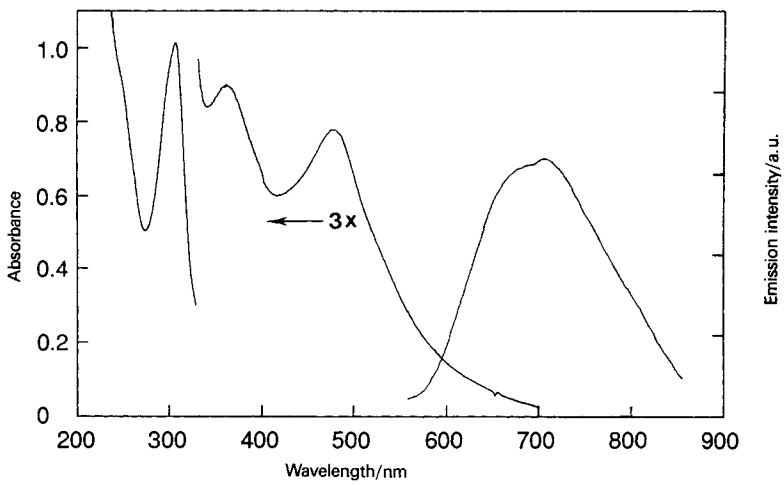

Fig. 5. *Absorption and emission spectrum of a* 10^{-5} M *solution of* **2** *in EtOH.* Optical pathlength 1 cm. Excitation wavelength for the luminescence 532 nm.

Electrochemical experiments employed an ethanolic solution of **1** and an aqueous solution of **2** (pH 3) in the presence of 0.2 M $LiClO_4$ as supporting electrolyte and a glassy carbon working electrode. H_2O was used as a solvent in the case of **2**, because of its low solubility in EtOH. Values for the standard redox potentials for the one-electron oxidation of **1** and **2** were determined as 0.68 and 0.73 V, respectively, measured *vs.* SCE. Values of E^0 were calculated by averaging the oxidative and reductive peak potentials.

Langmuir *Isotherms for Adsorption of* **1** *and* **2** *at the Surface of* TiO_2. Adsorption measurements employed solutions of **1** or **2** in EtOH containing 0.25 g/L TiO_2 powder (*Degussa P-25*, specific surface area 55 m^2/g) and 1×10^{-3} M HCl. Results are shown in *Fig. 6* where the data are fitted to a *Langmuir* isotherm. From the extrapolation of the straight lines, one obtains the binding constants $K_b = 4 \times 10^5 M^{-1}$ and $K_b = 2 \times 10^5 M^{-1}$ for **1** and **2**, respectively. These are high values for an adsorption constant implying strong interaction of the trinuclear complexes with the TiO_2 surface. From the K_b values, one derives adsorption standard free enthalpies of −0.33 eV and −0.31 eV for **1** and **2**, respectively.

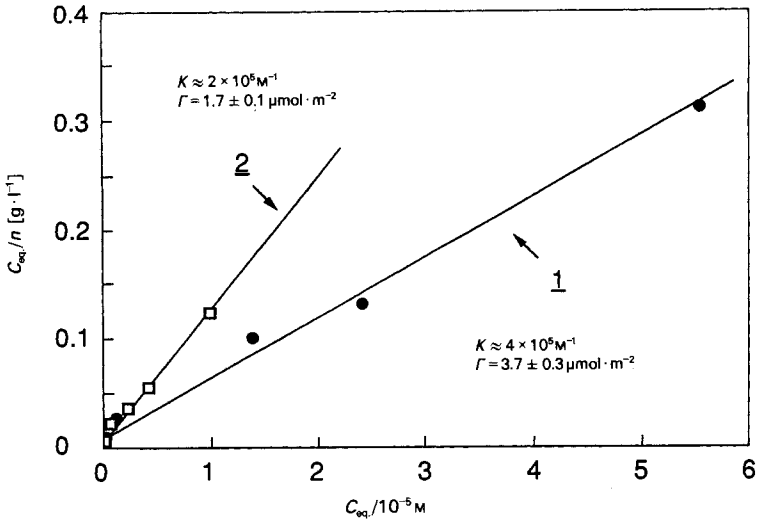

Fig. 6. *Isotherms for adsorption of* **1** *and* **2** *on* TiO_2 *(P-25, Degussa) powder dispersed in EtOH acidified with* 10^{-3} M *HCl.* Concentration of TiO_2: 0.25 g/l. Experimental data are plotted according to the *Langmuir* adsorption isotherm. The concentration of a trinuclear complex in solution at equilibrium divided by the number of moles of the complex adsorbed on 1 g of TiO_2 is plotted as a function of equilibrium concentration of **1** or **2**. K is the binding constant and Γ the surface concentration at monolayer coverage.

The surface area requirement is 45 ± 5 Å^2/molecule and 95 ± 8 Å^2/molecule for **1** and **2**, respectively, indicating that at saturation coverage there is twice as much **1** adsorbed on TiO_2 as **2**. This could arise from different configurations of the complexes in the adsorbed state. Since **2** has two carboxylic groups on all the bpy ligands, it might be attached to the TiO_2 surface *via* several COOH groups. As a result, this trimer is likely to be adsorbed in a flat configuration. The surface area occupied by **2** is comparable to that for the complex RuL_3 [14] which has been determined as 100 Å^2/molecule.

In contrast to **2**, **1** has only one Ru center with 4,4′-$(COOH)_2$-2,2′-bipy ligands. This could give rise to a more ordered array of adsorbed molecules: the central Ru atom may be attached to the surface of TiO_2 through the carboxylated ligands, the two peripheral moieties extending into the solution in an antenna-like fashion. Such a vertical alignment of adsorbate would allow for a higher packing density than a flat configuration. It should be noted, however, that the surface area of 45 Å^2/molecule derived for **1** from *Fig. 6* is smaller than the minimal space requirement for the trimeric complex, even if it is adsorbed in a vertical fashion with respect to the surface. Such a small area corresponds to an average distance between adjacent adsorbate molecules of only 6.7 Å. This could only be accomplished by significant stacking of **1** on the surface leading to energetically unfavorable intermolecular overlap of 2,2′-bpy ligands.

A plausible explanation of the data obtained for **1** in *Fig. 6* is that its adsorption on the TiO_2 particles exceeds monolayer coverage. For example, a bilayer of **1** may be formed through hydrophobic interaction of the 2,2′-bpy moieties of the complex. This is supported by luminescence analysis performed with TiO_2 particles after equilibration with ethanolic (2×10^{-5} M) solution of **1** and **2** for 16 h. Prior to analysis, the powder was

filtered, washed, and dried on a millipore filter. The emission of TiO_2 particles covered with **2** was barely discernable from the background in the 500 to 800 nm region. In contrast, TiO_2 powder onto which **1** was deposited exhibited significant luminescence with a distinct maximum around 650 nm. The appearance of the emission of **1** is rationalized in terms of multilayer adsorption. If the adsorption of the trinuclear complexes would be restricted to monolayer coverage, practically no luminescence could be detected due to the very efficient electron-transfer quenching by the TiO_2 substrate.

Laser Photolysis Investigations of Sensitized Charge Injection into Colloidal TiO_2. Investigations were performed with solutions of **1** or **2** in deaerated EtOH in the presence

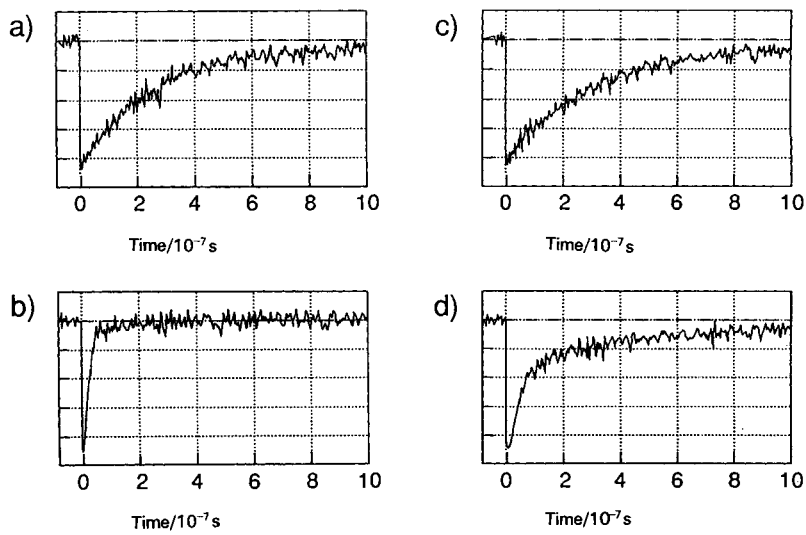

Fig. 7. *Effect of colloidal TiO_2 on the luminescence decay of* **1** *and* **2** *in acidic* (10^{-3} M HCl) *EtOH. a) b)* Oscilloscope traces showing the decay of the emission of **1** at 670 nm in the absence and presence of 1 g/l colloidal TiO_2, respectively. *c) d)* Oscilloscope traces showing the emission decay of **2** (6.0×10^{-6} M) at 650 nm in the absence and presence of 1 g/l colloidal TiO_2, respectively.

Table 1. *Absorption, Luminescence, and Electrochemical Properties of the CN-Bridged Trinuclear Ru Complexes*

Complex[a])	Abs. max. [nm] ($\varepsilon/10^4$ [$M^{-1} \cdot cm^{-1}$])	Emission maxima	Emission lifetime τ [ns]	E^{o}[b])
$[Ru^{II}L_2\{(CN)_2Ru^{II}L'_2\}_2]$	518 (sh) (1.56) 478 (1.88) 357 (2.01) 290 (8.83) 244 (6.12)	720 nm	320	0.68
$[Ru^{II}L_2\{(CN)_2Ru^{II}L_2\}_2]$	480 (2.90) 360 (3.34) 304 (11.26)	700 nm	330	0.73[c])

[a]) L = 4,4′-$(COOH)_2$-2,2′-bpy; L′ = 2,2′-bpy.

[b]) Average of anodic and cathodic peak potential for the first oxidation wave of the trinuclear complexes, determined by cyclic voltammetry, scan rate 10 mV/s, peak separation *ca.* 100 mV, reference electrode SCE.

[c]) Measured in H_2O at pH 3.2.

of 1 g/l colloidal TiO_2. The colloidal particles were prepared as described in the *Experimental*. To prevent precipitation of the colloid, the solution was acidified with 10^{-3} M HCl.

Fig. 7 illustrates the effect of colloidal TiO_2 on the luminescence decay of **1** and **2**. In the absence of TiO_2, the 670-nm emission of **1** decays in an exponential fashion with a lifetime of 320 ns, as reported in *Table 1*. Addition of the colloidal particles reduces sharply the luminescence lifetime. The decay occurs here so rapidly that it is completed within the duration of the laser pulse ($\tau < 10$ ns). A similar behavior is observed with ethanolic solutions of **2**. However, in this case the decay of emission at 650 nm is biphasic. The fast component comprising at least 60% of the total signal is followed by a slower decay whose lifetime is similar to that observed in TiO_2-free EtOH. The latter is attributed to the fraction of **2** that remains in solution and is not associated with the TiO_2 particles. These results show that the luminescence of the trinuclear complexes is strongly quenched upon association with the TiO_2 particles. They confirm moreover that **1** is more strongly adsorbed on the TiO_2 surface than **2**.

In *Fig. 8*, the products of this quenching process are identified by transient absorption spectroscopy. The end of pulse spectra for both **1** and **2** exhibit a bleaching signal in the vicinity of the absorption maxima of the trinuclear complexes, and an absorption that

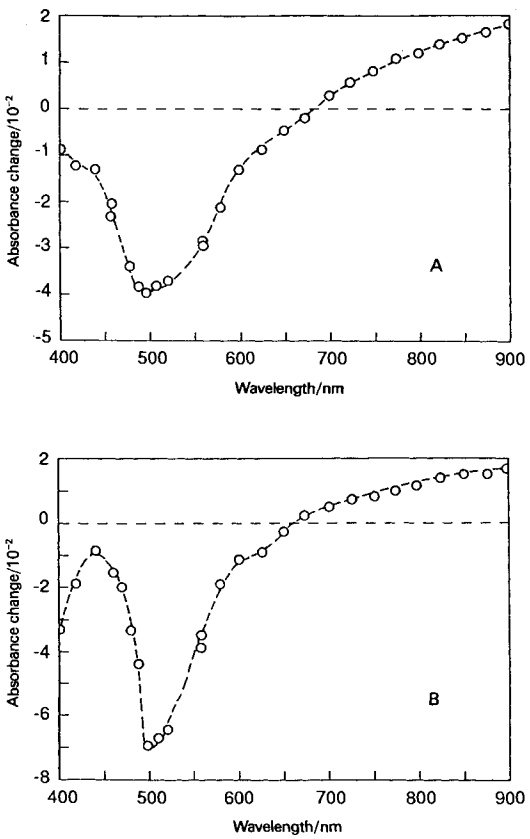

Fig. 8. *End of pulse spectra obtained from the 530-nm laser photolysis of ethanolic solutions containing 1 g/l TiO_2, 10^{-3} M HCl, and:* **1** (6.0×10^{-6} M) (*A*) *or* **2** (7.1×10^{-6} M) (*B*). Solutions were deaerated with Ar.

rises continuously towards the red. The absorption arises from both conduction band electrons and the oxidized forms of the trinuclear complex produced by photosensitized electron injection:

$$\mathbf{1}\,(\mathbf{2}) + h\nu \rightarrow \mathbf{1}^*\,(\mathbf{2}^*) \longrightarrow \mathbf{1}^+\,(\mathbf{2}^+) + e_{cb}^-\,(TiO_2) \qquad (2)$$

This process is so fast that it occurs concomitantly and within the 10-ns duration of the laser pulse. Picosecond techniques will be required to derive the rate constant of the charge injection process.

The spectrum of the conduction band electrons in colloidal TiO_2 particles has been previously investigated [15]. It exhibits a broad featureless band extending over much of the VIS into the IR region with a maximum around 700 nm. The extinction coefficient at 900 nm has been determined as 700 $M^{-1} \cdot cm^{-1}$. The oxidized trimers were produced independently by illuminating a 2×10^{-5} M aqueous solution (pH 2) of **1** and **2** in the presence of 10^{-2} M $Na_2S_2O_8$. Light-induced electron transfer from the trinuclear complexes to peroxodisulfate was found to proceed according to the equations:

$$\mathbf{1} + 1/2\ S_2O_8^{2-} + h\nu \longrightarrow [Ru(III)L_2(\mu\text{-}(CN)Ru(II)(CN)L_2')_2] + SO_4^{2-} \qquad (3)$$

$$\mathbf{2} + 1/2\ S_2O_8^{2-} + h\nu \longrightarrow [Ru(III)L_2(\mu\text{-}(CN)Ru(II)(CN)L_2)_2] \qquad (4)$$

The spectra of the one-electron oxidation products of **1** and **2** generated in this fashion show a broad band rising towards the IR with a maximum at around 1200 nm. This agrees with the reported [10] spectral features of the unsubstituted analogue $[Ru(III)L_2'(\mu\text{-}(CN)Ru(II)(CN)L_2')_2]$ where L′ = 2,2′-bpy. The extinction coefficients at 900 nm of the mixed valency trimers $[Ru(III)L_2(\mu\text{-}(CN)Ru(II)(CN)L_2')_2]$ ($\mathbf{1}^+$) and $[Ru(III)L_2(\mu\text{-}(CN)Ru(II)(CN)L_2)_2]$ ($\mathbf{2}^+$) were determined as 4100 $M^{-1} \cdot cm^{-1}$ and 4300 $M^{-1} \cdot cm^{-1}$, respectively. For the unsubstituted analogue, the extinction coefficient is 5000 $M^{-1} \cdot cm^{-1}$ [10].

The quantum yield of photosensitized electron injection was derived from the end of pulse spectra in *Fig. 8* as follows: first, the assumption was made that, at the laser intensities applied in *Fig. 8* all the sensitizer molecules present are photoexcited[1]). The fraction of excited sensitizer undergoing oxidative quenching according to *Eqn. 2* was then obtained from the bleaching signal at 560 nm, using as extinction coefficient the value determined for **1** and **2** in EtOH in the presence of 1 g/l colloidal TiO_2 and 10^{-3} M HCl. This fraction corresponds to the quantum yield for charge injection. The values obtained are $\Phi_{inj} = 0.63$ for **1** and $\Phi_{inj} = 0.43$ for **2**. In addition, the concentration of oxidized sensitizer and conduction band electrons produced during the laser pulse was calculated from the transient absorption signal obtained at 900 nm. The charge-injection quantum yields obtained from the transient absorption at 900 nm are in very good agreement with those derived form the 560 nm bleaching as shown in *Table 2*.

These quantum yields are significantly lower than the IPCE shown for these trinuclear complexes in *Fig. 1*. A similar behavior was recently observed for the mononuclear complex $[RuL_3]$ [3] [7]. The yield for photosensitized electron injection determined from

[1]) In this experiment, the laser power is increased, until the transient bleaching and absorption signal saturates; *cf.* [16].

Table 2. *Yields of Photo-induced Electron Injection Determined from Transient Absorption Changes Observed during Laser-Photolysis Studies of* **1** *and* **2** *in Colloidal TiO_2 Solution*

Complex	Additive	[S]/M	λ [nm]	Species	$\Sigma\varepsilon$ [$M^{-1} \cdot cm^{-1}$]	ΔA	ΔC [M]
1	–	6.0×10^{-6}	560	°S	8.0×10^3	-3.0×10^{-2}	-3.8×10^{-6}
	–	6.0×10^{-6}	900	S^+, e^-	4.8×10^3	1.8×10^{-2}	3.8×10^{-6}
	LI (10^{-1} M)	8.1×10^{-6}	560	°S	8.0×10^3	-4.4×10^{-2}	5.5×10^{-6}
	LI (10^{-1} M)	8.1×10^{-6}	900	S^+, e^-	4.8×10^3	2.5×10^{-2}	5.2×10^{-6}
	LI (10^{-1} M)	8.1×10^{-6}	900	e^-[a])	7.0×10^2	4.0×10^{-3}	5.7×10^{-6}
2	–	7.1×10^{-6}	560	°S	1.5×10^4	-4.8×10^{-2}	-3.2×10^{-6}
	–	7.1×10^{-6}	900	S^+, e^-	5.0×10^3	1.5×10^{-2}	3.0×10^{-6}
	LI (5×10^{-2} M)	8.0×10^{-6}	560	°S	1.5×10^4	-3.3×10^{-2}	-2.2×10^{-6}
	LI (5×10^{-2} M)	8.0×10^{-6}	900	S^+, e^-	5.0×10^3	1.7×10^{-2}	3.4×10^{-6}
	LI (5×10^{-2} M)	8.0×10^{-6}	900	e^-[a])	7.0×10^2	2.4×10^{-3}	3.4×10^{-6}

[a]) Measured 5 μs after the pulse; all other concentrations were determined immediately after the pulse.

colloidal solutions was also lower than the IPCE. Because the IPCE is composed of three terms, *i.e.*:

$$\text{IPCE} = \text{LHE} \times \Phi_{inj} \times P_{esc} \tag{5}$$

where LHE is the light-harvesting efficiency and P_{esc} is the probability that the injected electrons escape from recombination, one would expect the opposite result, *i.e.* the IPCE should be smaller than Φ_{inj}. However, we have recently observed that Φ_{inj} depends on the electrostatic potential of the TiO_2 film. Biasing the TiO_2, a few hundred millivolts positive from the flat band potential was found to increase the quantum yield for charge injection from 0.63 to 0.95 [17]. A similar increase is likely to occur in the sensitization of TiO_2 by **1** and **2**. Because the electric field in the colloidal particles is small, the conditions in *Fig. 8* are similar to that of a TiO_2 electrode at flat band potential. By contrast, in *Fig. 1* the TiO_2 electrode was employed in a regenerative cell containing an alcoholic I_2/I^- redox electrolyte. In such a configuration, the TiO_2 film is subjected to an anodic bias of 0.1 V (SCE), generating a depletion-layer field. This assists the electron transfer from the excited state of the trinuclear complex to the conduction band of the semiconductor increasing Φ_{inj}.

The following section will deal with the fate of the electrons injected in the colloidal TiO_2 particles. In particular, we shall examine the dynamics of charge recombination, *i.e.* the recapture of the conduction band electrons by the parent sensitizer ions:

$$\mathbf{1}^+ (\mathbf{2}^+) + e^-_{cb} (TiO_2) \longrightarrow \mathbf{1}\ (\mathbf{2}) \tag{6}$$

Fig. 9 shows oscillograms from the laser photolysis of colloidal solutions of **1** (7.3×10^{-5} M) in EtOH containing 1 g/l colloidal TiO_2 and 1×10^{-3} M HCl. The dashed curves were obtained in the presence of LiI (0.1M and 0.05M for **1** and **2**, respectively). The vertical rise in the 900 nm absorption is due to formation of $\mathbf{1}^+$ ($\mathbf{2}^+$) and e^-_{cb} (TiO_2) during the laser pulse. The subsequent decay of the absorption is biphasic: the major part decays within a few hundred ns, and this is followed by a tail extending into the ns time domain. The temporal behavior of the bleaching of the ground state absorption of **1** and **2** was also examined (*Fig. 9, a* and *c*) and was found to correspond to the mirror image of the transient absorption decrease. A computer fit of the fast decay to a first-order rate law yields, for the rate constant of intraparticle charge recombination, $k_b = 2.2 \times 10^7 s^{-1}$ and

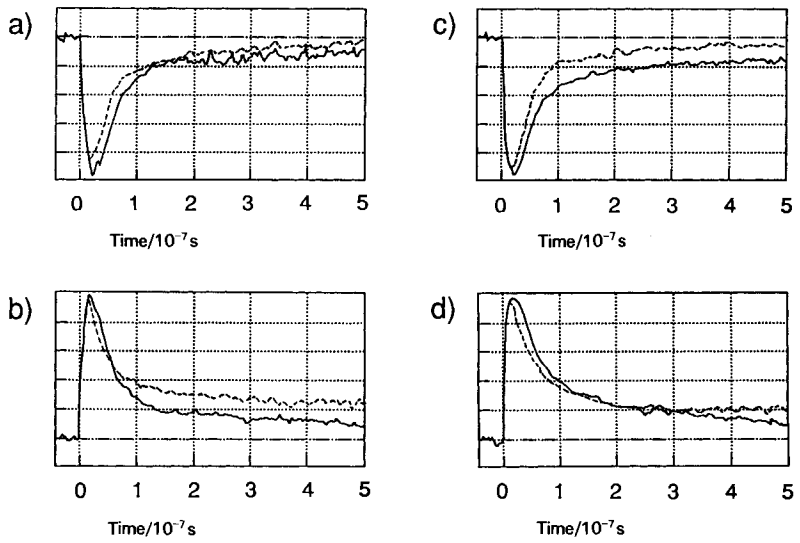

Fig. 9. *Oscilloscope traces obtained from the laser photolysis of trimeric Ru complexes in ethanolic solutions containing 1 g/l TiO_2 and 10^{-3} M HCl.* Conditions: *a) b)* 7.3×10^{-5} M solution of **1**; observation wavelength 560 nm and 900 nm, respectively. *c) d)* 7.1×10^{-5} M solution of **2**; observation wavelength 560 nm and 900 nm, respectively. The dashed lines represent oscilloscope traces obtained in the presence of LiI (concentration 0.1 M for *a* and *b* and 0.05 M for *c* and *d*).

$k_b = 1.4 \times 10^7 s^{-1}$ for **1** and **2**, respectively. For comparison, the value of k_b determined for the mononuclear analogue $[RuL_3]$ is $4 \times 10^5 s^{-1}$. This is 35–55 times smaller than the rate constant for the trinuclear complexes **1** and **2**.

To rationalize this difference, the *Marcus* theory [18] for nonadiabatic electron transfer is evoked which allows to express k_b in terms of H_{DA}, the electronic matrix coupling element, $\Delta G°$, the driving force of the back reaction, and λ the free energy of reorganization:

$$k_b = \frac{2\pi |H_{DA}|^2}{h\,(4\pi\lambda kT)^{1/2}} \exp[-(\Delta G° + \lambda)^2/(4\lambda kT)] \qquad (7)$$

The reactions considered here are all within the domain of the so-called inverted region where the rate of electron transfer is expected to decrease with increasing driving force. Because the redox potential of the trinuclear complexes is less positive than that of $[RuL_3]$, it is tempting to attribute the observed rate increase to a decrease in $\Delta G°$. In the case of the mononuclear complex $[RuL_3]$, the driving force of the back electron transfer is *ca.* −1.4 eV[2]). Since λ for trisbipyridine complexes of Ru is typically 0.5 eV [20], the exponential term has the value 9×10^{-8}. Using for the pre-exponential factor $10^{14} s^{-1}$, k_b is predicted to have a value around $9 \times 10^5 s^{-1}$ in reasonable agreement with the experiment. A factor of 50–55 in rate enhancement is readily accounted for by a relatively small

[2]) The driving force is estimated from the difference of the potential of the TiO_2, conduction band (*ca.* −0.2 V *vs.* NHE reference electrode at pH 3) and the redox potential of the deprotonated form of $[RuL_3]$ in aqueous solution (+1.2 V (NHE)). The latter may be slightly affected by adsorption of $[RuL_3]$ at the TiO_2 surface.

decrease of $\Delta G°$, *i.e.* from −1.4 to −1.3 eV[3]). Similar reasoning could explain the observation that the trinuclear complex $\mathbf{1}^+$ recaptures electrons from the conduction band somewhat faster than $\mathbf{2}^+$. For more detailed analysis, the reorganization energies of the trinuclear complexes in the adsorbed state are needed, and these will be determined from the temperature dependence of the electron-transfer rates.

Returning to *Fig. 9*, we next discuss the effect of iodide on the dynamics of the 560-nm bleaching recovery and 900-nm absorption decay. Iodide is an electron donor which reduces the oxidized state of the trinuclear complexes back to their original form:

$$1/2\,I^- + \mathbf{1}^+\,(\mathbf{2}^+) \longrightarrow \mathbf{1}\,(\mathbf{2}) + 1/2\,I_2 \qquad (8)$$

As a consequence, the recovery of the absorption of **1** and **2** is expected to be enhanced in the presence of I^-, and this is indeed borne out by the dashed oscilloscope traces in *Fig. 9, a* and *c*. The 900-nm signal decays also more rapidly, *Fig. 9, b* and *d*. However, in the presence of I^- the absorption reaches a plateau within a few hundred ns which is stable in deaerated solutions. This remaining signal arises from conduction-band electrons. *Table 2* shows that the concentration of e_{cb}^- (TiO_2) present after 5 μs is practically the same as that of the charge carriers produced during the laser pulse indicating that 0.05 or 0.1 M I^- suffices to intercept quantitatively the back reaction. One concludes from this observation that the rate constant of *Reaction 8* is close to the diffusion controlled limit which, for 5-nm sized particles, is predicted from the *Smoluchowski* equation to be $5.5 \times 10^{10}\,M^{-1} \cdot s^{-1}$ neglecting *Coulombic* effects.

Comparison of the Performance Characteristics of **1** *and* **2** *in Regenerative Photovoltaic Cells. Fig. 10* compares the current voltage characteristics of regenerative cells based on **1** and **2** as sensitizers. The same sandwich-type configuration was used as in *Fig. 1*. It consists of the dye-coated TiO_2 film deposited on conducting glass as photo-anode separated from the counterelectrode by a thin layer of EtOH containing 0.5 M LiI and

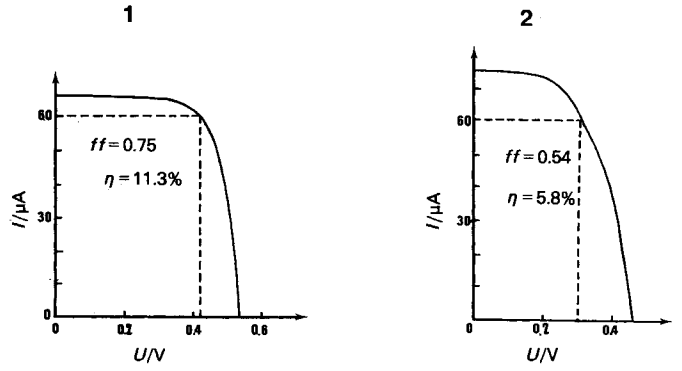

Fig. 10. *Photocurrent-voltage characteristics of thin layer regenerative photovoltaic cells consisting of the TiO_2 coated with trinuclear Ru complex, supported on a conducting glass sheet. 1:* Electrode surface area 1.4 cm^2, light intensity 1.6 W/m^2; *2:* area 1.7 cm^2, light intensity 1.83 W/m^2; other conditions as in *Fig. 1*. The efficiencies reported refer to incident light and are uncorrected for the *ca.* 20% fraction of light absorbed or reflected by the conducting glass support.

[3]) The decrease in the driving force for back electron transfer could be due to the fact that the redox potential for one-electron oxidation of **1** or **2** is lower than that of $[RuL_3]$.

3×10^{-3} M I_2. Monochromatic light of 520 nm wavelength was used to excite the dye-coated TiO_2 film. Irradiation was performed from the front side through the conducting glass support. Efficiencies quoted refer to incident light intensities and are uncorrected for light reflection, scattering, and absorption (together *ca.* 20% at 520 nm) by the glass sheet.

The TiO_2 film coated with **1** gave a short circuit photocurrent of $i_{sc} = 46$ μA/cm² at an incident light intensity of 1.6 W/m² corresponding to a IPCE value of 69%. As the load resistance or voltage is increased, the current at first stays fairly constant and then falls to zero at an open circuit voltage of $V_{oc} = 0.53$ V. (The open circuit voltage increased with light intensity; in sunlight V_{oc} was *ca.* 0.8 V.) The maximum power delivered is represented by the area of the largest rectangle that can be fitted under the curve: in *Fig. 10* 180 mW/m² at 0.44 V. Dividing this by the product $V_{oc} \times i_{sc}$ gives the fill factor (*ff*) of the cell for which a value of 0.75 is obtained. Such a value is strikingly high for a device based on a polycrystalline semiconductor film, since it is comparable to *ff* value achieved with top quality single crystal photovoltaic cells. The power conversion efficiency (η) at 520 nm, *i.e.* the maximum power output expressed as a percentage of input light power, is 11.3%.

For **2** as a sensitizer, $i_{sc} = 44$ μA/cm² at 1.83 W/m² incident light intensity corresponding to IPCE = 58%. $V_{oc} = 0.47$ V, *ff* = 0.54, and $\eta = 5.8\%$.

These data indicate that the performance characteristics of **2** are inferior to **1**. This could be due to several factors that are presently being investigated. Electrochemical experiments performed with dye-loaded TiO_2 films have shown the reduction of triiodide by e_{cb}^- (TiO_2):

$$2e_{cb}^- (TiO_2) + I_3^- \longrightarrow 3I^- \qquad (9)$$

to play an important role in influencing the performance characteristics of the cell. For example, the V_{oc} was found to be to a large degree determined by the kinetics of this reaction. Similar effects have been observed with conventional photoelectrochemical cells, and a kinetic interpretion of V_{oc} has been published by *Lewis* and coworkers [20]. *Reaction 9* manifests itself by an enhancement of the cathodic dark current in the presence of triiodide, and this was found to be significantly smaller with **1** as compared to **2**. It is inferred from this observation that **1** is more effective in preventing leakage current from the conduction band of the semiconductor to I_3^- than **2**. Thus, there are subtle but important differences in the interaction of these two trinuclear complexes with TiO_2 which affect the ease of access of the I_3^- to the surface. This is corroborated by the fact that the *Langmuir* adsorption constant for **1** is twice as large as that for **2**, and that there is more **1** adsorbed at the surface than **2**. The pronounced red shift in the absorption spectrum of **1** accompanying the adsorption process underlines further its strong electronic interaction with the support.

Long-Term Stability of **1** *under Photoinduced Redox Cycling.* A TiO_2 film (area 3.9 cm²) was coated with **1** (*ca.* 2×10^{-8} mol/cm²) and immersed in a cell containing alcoholic I_2/I^- redox electrolyte. It was subjected to white light illumination for one month, until the electric charge that passed through the cell was 4260 C/cm². No significant decline in photocurrent was noted over this period during which the trinuclear complex had been turned over 2×10^6 times. This is an encouraging result which indicates that the sensitizer can sustain long-term redox cycling, rendering it a promising candidate for application in a practical photovoltaic device.

This work was supported by the *Swiss National Science Foundation* and the *Office Fédéral pour l'Energie.*

REFERENCES

[1] H. Gerischer, *Angew. Chem.* **1988,** *100,* 630.

[2] a) H. Meier, *J. Phys. Chem.* **1965,** *69,* 724; b) K. Hauffe, J. Range, *Z. Naturforsch., B* **1968,** *238,* 736; c) T. Watanabe, A. Fujishima, K. Honda, in 'Energy Resources Through Photochemistry and Catalysis', Academic Press, New York, 1983; d) H. Tributsch, M. Calvin, *Photochem. Photobiol.* **1971,** *14,* 95; e) P. V. Kamat, M. A. Fox, *Chem. Phys. Lett.* **1983,** *102,* 379; f) R. Memming, *Progr. Surf. Sci.* **1984,** *17,* 7; g) M. Krishnan, X. Zhang, A. J. Bard, *J. Am. Chem. Soc.* **1984,** *106,* 7371; h) H. Gerischer, F. Willig, *Topics Curr. Chem.* **1976,** *61,* 31; i) K. Hashimoto, *J. Phys. Chem.* **1986,** *90,* 4474; k) M. Spitler, *J. Electroanal. Chem.* **1987,** *228,* 69. For related work, *cf.*: D. F. Blossey, *Phys. Rev.* **1974,** *139,* 5183; F. Willig, *Chem. Phys. Lett.* **1976,** *40,* 331; l) K. Bitterling, F. Willig, *J. Electroanal. Chem.* **1986,** *204,* 211; m) M. A. Ryan, E. C. Fitzgerald, M. T. Spitler, *J. Phys. Chem.* **1989,** *93,* 6150; n) J. Moser, M. Grätzel, *J. Am. Chem. Soc.* **1984,** *106,* 6557.

[3] J. Desilvestro, M. Grätzel, L. Kavan, J. Moser, J. Augustynski, *J. Am. Chem. Soc.* **1985,** *107,* 2988.

[4] K. Kalyanasundaram, N. Vlachopoulos, V. Krishnan, A. Monnier, M. Grätzel, *J. Phys. Chem.* **1987,** *91,* 2342.

[5] E. Vrachnou, N. Vlachopoulos, M. Grätzel, *J. Chem. Soc., Chem. Commun.* **1987,** 868.

[6] O. Enea, J. Moser, M. Grätzel, *J. Electroanal. Chem.* **1989,** *259,* 59.

[7] N. Vlachopoulos, P. Liska, J. Augustynski, M. Grätzel, *J. Am. Chem. Soc.* **1988,** *110,* 1216.

[8] P. Liska, N. Vlachopoulos, M. K. Nazeeruddin, P. Compte, M. Grätzel, *J. Am. Chem. Soc.* **1988,** *110,* 3686.

[9] W. T. Wu, A. J. McEvoy, M. Grätzel, submitted to *J. Electroanal. Chem.*

[10] a) C. A. Bignozzi, S. Roffia, C. Chiorbolli, J. Davila, M. T. Indelli, F. Scandola, *Inorg. Chem.* **1989,** *28,* 4350, and ref. cit. therein; b) J. N. Demas, T. F. Turner, G. A. Crosby, *Inorg. Chem.* **1969,** *8,* 674.

[11] F. Scandola, oral presentation at 'Eight International Symposium on the Photochemistry and Photophysics of Coordination Compounds', Univ. of California, Santa Barbara, USA, Aug. 13–17, 1989. Since then, a manuscript has been submitted for publication by R. Amadelli, R. Argazzi, C. A. Bignozzi, F. Scandola.

[12] G. Rothenberger. P. P. Infelta, M. Grätzel, *J. Phys. Chem.* **1979,** *83,* 1871.

[13] D. A. Gulino, H. G. Drickamer, *J. Phys. Chem.* **1984,** *88,* 1173.

[14] D. N. Furlong, D. Wells, W. H. F. Sasse, *J. Phys. Chem.* **1986,** *80,* 1107.

[15] U. Kölle, J. Moser, M. Grätzel, *Inorg. Chem.* **1985,** *24,* 2253.

[16] U. Lachish, P. P. Infelta, M. Grätzel, *Chem. Phys. Lett.* **1979,** *62,* 317.

[17] B. O'Regan, M. Anderson, J. Moser, M. Grätzel, submitted to *J. Phys. Chem.*

[18] R. A. Marcus, N. Sutin, *Biochim. Biophys. Acta* **1985,** *811,* 265.

[19] N. Sutin, in 'Tunneling in Biological Systems', Eds. P. Chance, D. C. Devault, J. R. Schriffer, H. Frauenfelder, and H. Sutin, Academic Press, New York, 1979.

[20] S. R. Lunt, L. G. Casagrande, B. J. Tufts, N. S. Lewis, *J. Phys. Chem.* **1988,** *92,* 5766.